Published online February 12, 2004

916–925 *Nucleic Acids Research, 2004, Vol. 32, No. 3*
DOI: 10.1093/nar/gkh250

Kinetic and thermodynamic characterization of the RNA-cleaving 8-17 deoxyribozyme

Maria Bonaccio, Alfredo Credali and Alessio Peracchi*

Department of Biochemistry and Molecular Biology, University of Parma, 43100 Parma, Italy

Received October 27, 2003; Revised and Accepted January 5, 2004

ABSTRACT

The 8-17 deoxyribozyme is a small DNA catalyst of significant applicative interest. We have analyzed the kinetic features of a well behaved 8-17 construct and determined the influence of several reaction conditions on such features, providing a basis for further exploration of the deoxyribozyme mechanism. The 8-17 bound its substrate with a rate constant ~10-fold lower than those typical for the annealing of short complementary oligonucleotides. The observed free energy of substrate binding indicates that an energetic penalty near to +7 kcal/mol is attributable to the deoxyribozyme core. Substrate cleavage required divalent metal ion cofactors, and the dependence of activity on the concentration of Mg^{2+}, Ca^{2+} or Mn^{2+} suggests the occurrence of a single, low-specificity binding site for activating ions. The efficiency of activation correlated with the Lewis acidity of the ion cofactor, compatible with a metal-assisted deprotonation of the reactive 2′-hydroxyl group. However, alternative roles of the metal ions cannot be excluded, because those ions that are stronger Lewis acids are also capable of forming stronger interactions with ligands such as the phosphate oxygens. The apparent enthalpy of activation for the 8-17 reaction was close to the values observed for hydroxide-catalyzed and hammerhead ribozyme-catalyzed RNA cleavage.

INTRODUCTION

While the functional versatility and the catalytic aptness of proteins and RNA have been appreciated for a long time, the biological functions of DNA are assumedly limited to the storage and transmission of genetic information, and catalytic DNA molecules have not yet been isolated from living organisms. Despite this, a large number of *in vitro* selection studies have shown that single-stranded DNA, much like single-stranded RNA, can fold into complex tertiary structures and perform molecular recognition and catalysis (reviewed in 1–3). In particular, the discovery of catalytic DNAs, or deoxyribozymes, has raised great interest in different scientific areas. From a mechanistic standpoint, enzymes made of DNA are convenient model systems in which the molecular basis of nucleic acid catalysis can be investigated. From an applicative standpoint, deoxyribozymes show advantageous features, such as chemical stability, ease of synthesis and amenability to rational design, that make them particularly suited for many biotechnological and pharmaceutical uses.

An especially relevant example is provided by two small RNA-cleaving deoxyribozymes, termed ‘8-17’ and ‘10-23’, originally identified by Santoro and Joyce (4). These deoxyribozymes can be designed to recognize and cleave specific RNA targets (e.g. viral mRNAs), and are thus being investigated as potential chemotherapeutics (5,6). Moreover, these catalysts have found use in a variety of applications, ranging from the analysis and quantification of nucleic acids (7,8) to the preparation of homogeneous RNA transcripts (9,10) and from analytical biotechnology (11,12) to the development of molecular-scale computational devices (13,14).

Optimal usage of the RNA-cleaving deoxyribozymes implies an understanding of their kinetic and thermodynamic characteristics, as well as knowledge of the influence of the reaction conditions on these features. Although several detailed works have examined the kinetic behavior and the general functional properties of the 10-23 DNA enzyme (15–22), our knowledge of the 8-17 deoxyribozyme is much more limited (23–25).

Here, we report a functional characterization of the 8-17 motif, addressing the kinetic and mechanistic features of the RNA-cleavage reaction it catalyzes. Besides helping to optimize deoxyribozyme applications, this work allows a meaningful comparison of the properties of 8-17 with the better known 10-23 deoxyribozyme and with small catalytic RNAs, in particular the hammerhead ribozyme. Furthermore, our results yield some insights into the basis of the deoxyribozyme function, and provide a foundation for future mechanistic studies.

MATERIALS AND METHODS

Materials

DNA oligonucleotides were purchased from MWG Biotech (Ebersberg, Germany). RNA and RNA–DNA mixed oligonucleotides were from Dharmacon Research (Lafayette, CO). When necessary, chemically synthesized oligonucleotides were ^{32}P-5′-end-labeled with T4 polynucleotide kinase. Concentrations of radioactive oligonucleotides were determined from specific activities; concentrations of non-radioactive oligonucleotides were determined using extinction

*To whom correspondence should be addressed. Tel: +39 0521905137; Fax: +39 0521905151; Email: alessio.peracchi@unipr.it

coefficients at 260 nm estimated by the nearest neighbor method (26).

1,4-Piperazinediethane sulfonic acid (PIPES) was purchased from Fluka. 1,3-Bis[tris(hydroxymethyl)methylamino]propane (Bis-tris propane) was from Sigma. Unless otherwise stated, measurements were carried out in 50 mM PIPES–NaOH, adjusted to pH 7.4 at the final reaction temperature. The ionic strength was adjusted to ~0.21 M with NaCl (e.g. 75 mM NaCl for reactions to be carried out at 37°C). For reactions to be carried out at low metal ion concentrations, the buffer solutions were treated beforehand with microspheres of a chelating resin (Chelex 100, Sigma) to remove any contaminating divalent metal ions.

Divalent metal chlorides (>99.99%) were from Aldrich. Solutions of transition metal chlorides were used immediately after preparation to minimize metal oxidation or formation of insoluble hydroxides.

Constructs used

We used two different 8-17 deoxyribozyme constructs, termed (8-17)*cb* and (8-17)*q*, respectively (Fig. 1A). In both constructs, the catalytic core contains a 'TCGAA' unpaired region, instead of the 'ACGA' turn present in the 'canonical' 8-17 motif (4)—this change renders the 8-17 motif more active in the presence of Mg^{2+} and Mn^{2+}, while reducing its preference for Ca^{2+} versus Mg^{2+} as a metal ion cofactor (24). Both deoxyribozymes have substrate-binding arms of identical length (7 nt in the 5′ arm, 8 nt in the 3′ arm) and recognize 17mer substrates that are predicted to possess no secondary structure at room temperature. The two substrates have completely different sequences, even though they both contain nine G+C nucleotides.

Test of the conformational homogeneity of (8-17)*cb*

Non-denaturing gel electrophoresis was used to check for the occurrence of alternative conformations in the (8-17)*cb* system (27). Labeled and non-labeled oligonucleotides were mixed in PIPES–NaOH/pH 7.4, heated at 95°C for 2 min and allowed to cool at room temperature before adding glycerol (5% final) and loading on the gel. Electrophoresis was carried out on 18% acrylamide gels (20 × 30 × 0.1 cm) in 50 mM Tris-acetate (pH 7.5) containing 3 mM Mg^{2+} acetate. The gels were run at 10 W for ~10 h, at room temperature. Both the free (8-17)*cb* deoxyribozyme and its free substrate (at concentrations up to 4 μM) migrated as a single band, excluding the occurrence of slowly interconverting conformations that might affect the kinetic analysis (27). Similarly, the annealed deoxyribozyme–substrate complex migrated as a single band under these conditions.

General kinetic methods

Substrate and deoxyribozyme were separately heated at 95°C for 2 min to disrupt potential aggregates, spun briefly in a microfuge and equilibrated for 10 min at the reaction temperature, in a thermostated water bath. After adding the desired concentration of divalent metal ions to the deoxyribozyme tube, reactions were initiated by adding the substrate (total volume of the reaction mixture: 40 μl). Time-points were collected at appropriate intervals and quenched by adding formamide and excess EDTA. Radiolabeled substrates and products were separated on 7 M urea/20% polyacrylamide gels and quantitated using a Personal Molecular Imager (Bio-Rad). Reaction time-courses were fit to the appropriate kinetic equation using Sigma Plot (SPSS Inc.).

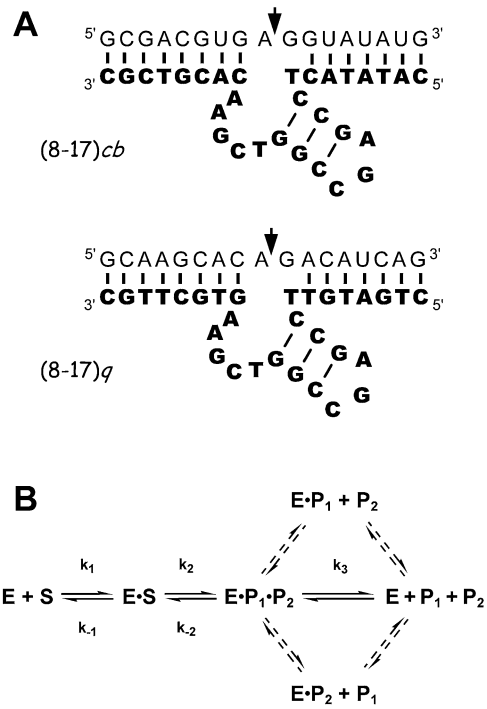

Figure 1. (**A**) Primary and secondary structures of the 8-17 constructs used in this study. The DNA enzymes are shown in bold letters and their RNA substrates are shown in normal letters. The arrows indicate the sites of cleavage. (**B**) Kinetic scheme for the RNA cleavage reaction carried out by the 8-17 deoxyribozyme. The DNAzyme (E) binds to its substrate (S), forming a productive bimolecular complex (E·S). Subsequently, S is cleaved to yield two products: P1 (containing a cyclic 2′,3′-phosphate) and P2 (containing a free 3′-hydroxyl) (4). P1 and P2 can dissociate with different rates and in different orders (dashed arrows); in general, however, only release of the product that dissociates most slowly affects multiple-turnover catalysis. This rate is represented here by k_3.

Multiple turnover reactions

For reactions carried out under multiple-turnover conditions, the total concentration of substrate, [S], was always >10-fold in excess over the total concentration of enzyme, [E]. The reaction rate (v_{obs}) was obtained for each [S] from a linear fitting of the data points collected over the first 10–20% of the reaction. Cleavage rates were measured at nine different concentrations of substrate, typically ranging from ~6-fold below to ~10-fold above K_M. k_{cat} and K_M values were determined by non-linear least-squares fitting a plot of v_{obs}/[E] versus [S] to the following form of the Michaelis–Menten equation:

$$\frac{v_{obs}}{[E]} = \frac{k_{cat}[S]}{K_M + [S]} \quad \mathbf{1}$$

Measurement of the rate constant for substrate cleavage (k_2)

k_2 (the rate constant for cleavage within the enzyme–substrate complex) was measured under single-turnover conditions, so

that release of the product could not affect the observed rate. In our experiments, the reaction was started by mixing a trace of labeled substrate (~0.1 nM) with ⩾1 μM E (final concentration). Two controls ensured that, under these conditions, substrate binding was not rate limiting. First, the measured rate constants remained identical, within error, when the deoxyribozyme concentration was raised from 1 to 10 μM. Second, for reaction conditions in which cleavage was particularly fast, a different order of addition was also tested: the deoxyribozyme and the substrate were heat-treated together in 36 μl of PIPES–NaOH buffer, allowed to anneal 10 min at the desired reaction temperature and finally supplemented with 4 μl of metal chloride to initiate the reaction. The observed rate constants obtained this way were indistinguishable from those obtained through the standard reaction protocol.

Cleavage reactions with rate constants $>10^{-3}$ min^{-1} were followed to completion; the resulting reaction time-courses fit well to a single-exponential function ($R^2 > 0.99$), with no lags or multiple phases, and endpoints typically between 80 and 90%. Slower reactions were followed for at least 40 h and rate constants were determined from the initial rates, assuming an endpoint of 90%. The time-courses of these slow reactions provided no indication for time-dependent inactivation of the deoxyribozyme.

Measurement of the substrate dissociation rate constant (k_{-1})

Pulse–chase experiments (15,28) were used to compare the rate of deoxyribozyme–substrate dissociation, k_{-1}, with the rate of substrate cleavage, k_2 in the presence of 3 mM Mg^{2+} (or Ca^{2+}) at 25°C.

In these experiments, a saturating concentration of deoxyribozyme (100 nM) was first allowed to bind a trace amount of radiolabeled S (~0.1 nM) for a period, t_1 = 4 min, in the presence of 3 mM metal ions (over this time, <4% of the substrate was cleaved). Then the reaction mixture was supplemented with a large excess of unlabeled substrate (1 μM final) to initiate the chase period, t_2, during which dissociation of labeled S from the deoxyribozyme was essentially irreversible. An otherwise identical reaction, but without the chase, was carried out in parallel. Partitioning of the labeled substrate between cleavage and release depended on the relative magnitude of k_{-1} and k_2; in particular, the final extent of cleavage in the presence of the chase mirrored the ratio $k_2/(k_{-1} + k_2)$ (29), so that knowing k_2 and the final extent of cleavage allowed k_{-1} to be determined.

Measurement of the substrate association rate constant (k_1)

A pulse–chase strategy was also used to determine the rate of enzyme–substrate association, k_1, in the presence of 3 mM Mg^{2+} or Ca^{2+}, at 25°C. In these experiments, an excess of deoxyribozyme (1–15 nM) was first allowed to bind a trace amount of radiolabeled substrate for a period, t_1, variable from 0.5 to 7 min (over this time, in the presence of Mg^{2+} or Ca^{2+}, <4% of the substrate was cleaved). Then the material was transferred into a solution that contained a large excess of unlabeled substrate (to prevent any further binding of radioactive substrate) as well as 15 mM Mn^{2+} pH 7.8. The high concentration of Mn^{2+} and the slightly increased pH ensured cleavage of all the bound labeled substrate within <3 min, so that the fraction of cleaved S reflected the amount of E·S formed at t_1. The dependence of such a fraction on t_1 could be fitted to a single exponential function, yielding a pseudo first-order rate constant for substrate binding, k_{obs}. k_1 was obtained by linear least-squares fitting the k_{obs} values as a function of [E].

Thermal denaturation studies

The thermal denaturation of the complex between the (8-17)*cb* deoxyribozyme and a non-cleavable substrate analog (containing a single deoxyribonucleotide at the cleavage site) was measured on a Perkin-Elmer Lambda Bio 20 spectrophotometer, equipped with a PTP-6 Peltier temperature programmer. Deoxyribozyme and substrate analog, in PIPES–NaOH, were heated together at 95°C for 2 min, then cooled at room temperature, supplemented when required with $MgCl_2$ and finally placed into the spectrophotometer and equilibrated at 10°C. Melting curves (absorbance versus temperature) were recorded by heating the samples (1°C/min) and following the UV signal variation at 260 nm. The exterior of the cuvette was kept under a stream of dry N_2 gas to prevent water condensation at low temperatures.

RESULTS

The 8-17 constructs used in this study are shown in Figure 1A. The (8-17)*cb* construct, which was described before (30) and which was tested for the absence of gross conformational heterogeneity (see Materials and Methods), is the main subject of this characterization study. The (8-17)*q* construct recognizes a very different substrate and has been employed as a control, to ensure that the observed features of (8-17)*cb* had a relevance to 8-17 deoxyribozymes in general.

A minimal kinetic scheme for the 8-17 reaction is shown in Figure 1B. The first step of the reaction is represented by binding of the catalytic DNA (E) to its substrate (S), to form a productive enzyme–substrate complex (E·S). The substrate is then cleaved and the two products are released to regenerate the free enzyme.

Limits for two of the rate constants depicted in Figure 1B can be obtained from the literature. It is known that, in the (8-17)*cb* system, the rate of product release is generally much faster than the rate of cleavage (30; see also below)—hence $k_3 >> k_2$. Also, it is known that the 8-17 deoxyribozyme is much less efficient in the ligation reaction than in cleavage (31)—hence $k_{-2} << k_2$. Based on these limits, and through a steady-state treatment, the scheme in Figure 1B predicts a Michaelis–Menten behavior, i.e. a hyperbolic dependence of the observed rate of cleavage on [S] (32), where:

$$k_{cat} = \frac{k_2 k_3}{k_2 + k_{-2} + k_3} \approx k_2 \qquad \mathbf{2}$$

and

$$K_M = \frac{k_2 k_3 + k_{-1} k_{-2} + k_{-1} k_3}{k_1 (k_2 + k_{-2} + k_3)} \approx \frac{k_2 + k_{-1}}{k_1} \qquad \mathbf{3}$$

In this work, we first measured the multiple-turnover kinetic parameters of the (8-17)*cb* construct, then the individual rate

Table 1. Catalytic parameters for the 8-17 reaction

Construct	Metal ion cofactor	T (°C)	k_{cat} (min^{-1})	K_M (nM)	k_{cat}/K_M (M^{-1} min^{-1})	k_2 (min^{-1})	k_1 (M^{-1} min^{-1})	k_{-1} (min^{-1})	K_S[a] (nM)
(8-17)*cb*	3 mM Mg^{2+}	37	0.019	50	4×10^5	0.020	–	–	–
		25	0.010	4	5×10^6	0.011	1.7×10^7	0.02	1.2
	3 mM Ca^{2+}	37	0.027	250	1×10^5	0.026	–	–	–
		25	0.014	7	2×10^6	0.018	1×10^7	0.04	4
	3 mM Mn^{2+}	37	0.67	80	8×10^6	0.8	–	–	–
		25	0.2	20	1×10^7	0.4	(5×10^7)[b]	–	–
(8-17)*q*	3 mM Mg^{2+}	25	0.019	2	1×10^7	0.021	3.3×10^7	0.005	0.15
	3 mM Ca^{2+}	25	0.026	1	2×10^7	0.025	–	0.007	–
	3 mM Mn^{2+}	25	0.22	10	2×10^7	0.3	–	–	–

Conditions: PIPES–NaOH buffer pH 7.4. Data are the average of at least two independent determinations.
[a]K_S represents the thermodynamic constant for substrate dissociation and is calculated as k_{-1}/k_1.
[b]This is the rate of association of (8-17)*cb* to an all-DNA substrate analog, measured in a previous study (30).

constants k_2, k_1 and k_{-1}, and finally we examined the specific effect of reaction conditions (such as the concentration of metal ion cofactors, pH and temperature) on the cleavage rate.

Measurement of the steady-state catalytic parameters

The multiple-turnover reaction carried out by the 8-17 deoxyribozyme was studied under conditions that approach the intracellular setting (i.e. ionic strength ~0.2 M, pH 7.4, 37°C and in the presence of 3 mM Mg^{2+}) but also at a different temperature (25°C) and/or in the presence of other divalent metal ions (Ca^{2+} and Mn^{2+}). The values of the observed kinetic parameters (k_{cat} and K_M) are summarized in Table 1. Similar to what was reported for the 10-23 deoxyribozyme (15), k_{cat} values measured in Mn^{2+} were 20- to 35-fold faster than k_{cat} values measured in Mg^{2+}.

Measurement of individual rate constants: k_2, k_1 and k_{-1}

As shown in Figure 2B, k_2 represents the rate constant for cleavage of the substrate within the E·S complex. This parameter was measured in single-turnover reactions, ensuring that the product dissociation step did not affect the observed kinetics. Under each of the temperature and ionic conditions examined, k_2 values for (8-17)*cb* were in remarkable agreement with the values of k_{cat} (Table 1), as predicted by equation **2**. This systematic coincidence confirms that multiple turnover is not limited by product release; in other words, k_3 is much greater than k_2 under all the reaction conditions tested (with the only possible exception of reactions carried out at 25°C, 3 mM Mn^{2+}).

The rate constants for substrate association and dissociation (indicated as k_1 and k_{-1}, respectively) were determined through the use of pulse–chase experiments, in the presence of 3 mM Mg^{2+} or 3 mM Ca^{2+}, at 25°C. The measured dissociation rates were substantially different for the (8-17)*cb* and the (8-17)*q* constructs, reflecting the different interactions of the two deoxyribozymes with their respective substrates.

On the other hand, substrate association in both the (8-17)*cb* and the (8-17)*q* system occurred with rate constants in the range 1–5 $\times$ 10^7 M^{-1} min^{-1} (Table 1). These values are comparable to the rate constants for association of (8-17)*cb* to an all-DNA substrate analog, measured through application of the 'ethidium assay' (30): the substrate analog bound with an apparent rate of 4×10^7 M^{-1} min^{-1} in the presence of 3 mM Mg^{2+} and 3×10^7 M^{-1} min^{-1} in the presence of 3 mM Ca^{2+} (D. Ferrari and A. Peracchi, unpublished results).

Dependence of k_2 on the concentration of Mg^{2+}, Mn^{2+} and Ca^{2+}

The rate of the cleavage step, k_2, was measured under single turnover conditions as a function of either [Mg^{2+}], [Ca^{2+}] or [Mn^{2+}] at 25°C (Fig. 2). In all three cases, the data could be described by a single, non-cooperative binding process, fitting well to a hyperbolic function of the type:

$$k_2 = \frac{k_{max}[M^{2+}]}{K_d + [M^{2+}]} \qquad \mathbf{4}$$

k_{max} indicates the value of k_2 in the presence of saturating divalent metal ion and K_d is the apparent dissociation constant for the metal ion. These simple hyperbolic titrations are remarkable because many metal ions are expected to bind to the negatively charged deoxyribozyme and because the ionic strength of the solution more than doubles when the concentration of divalent metal ion is raised from 0 to 100 mM—both of these factors, in principle, could give rise to substantially more complex dependences of activity on [M^{2+}].

The deoxyribozyme activity exhibited similar profiles when assayed as a function of either [Ca^{2+}] or [Mg^{2+}] (Fig. 2A and B). Both of these metals showed k_{max} values in the range 0.07–0.1 min^{-1}, and the apparent dissociation constants were 15 mM for Mg^{2+} and 8 mM for Ca^{2+}. In contrast, the observed k_{max} for Mn^{2+}-dependent cleavage was 1.3 min^{-1}, while half-maximal activity required the presence of only 4 mM Mn^{2+}.

Dependence of of k_2 on the type of added metal ions

Contrary to several small ribozymes (33), the 8-17 deoxyribozyme was not significantly active in the presence of monovalent cations alone. Cleavage in the presence of 4 M Li^+ or 4 M Na^+ was at least 10^3-fold lower than cleavage in the presence of 3 mM Mg^{2+} (i.e. <0.5% of the substrate was cleaved in 70 h).

On the other hand, Lu and coworkers have shown that 8-17 constructs are active in the presence of a variety of divalent metal ions (23,25). We thus assayed the rate of (8-17)*cb*-catalyzed RNA cleavage, k_2, at pH 7.4 in the presence of nine different divalent cations: the alkaline earth metal ions Mg^{2+}, Ca^{2+}, Sr^{2+}, Ba^{2+} and the transition metal ions Mn^{2+}, Co^{2+}, Zn^{2+}, Cd^{2+} and Ni^{2+}. The ions Cu^{2+} and Sn^{2+} did not support the 8-17 activity under our reaction conditions. Furthermore, although Pb^{2+} ions are extremely efficient activators of the

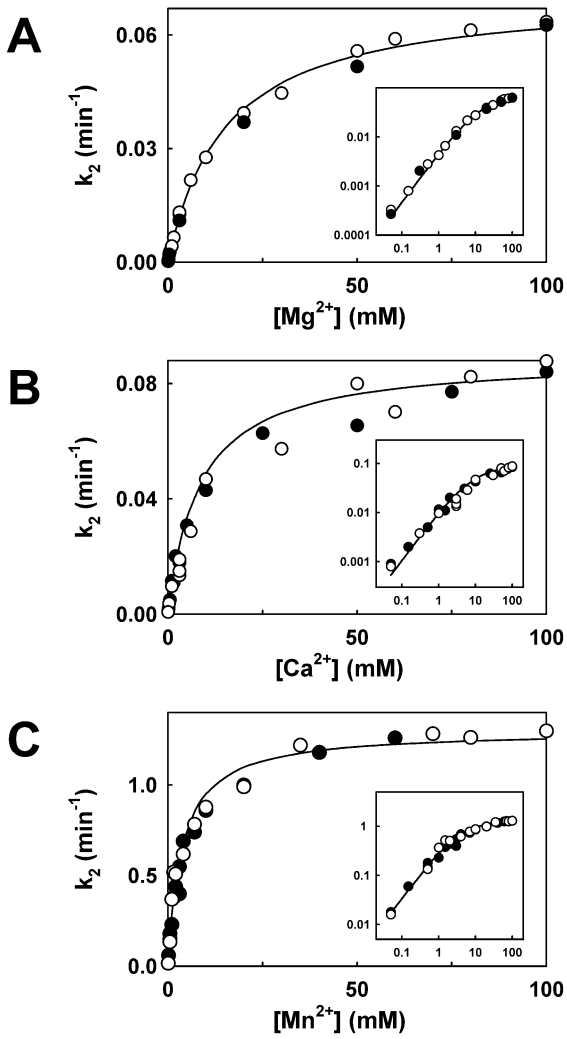

Figure 2. Dependence of k_2 on the concentration of either Mg^{2+} (**A**) or Ca^{2+} (**B**) or Mn^{2+} (**C**). Reactions were carried out using the (8-17)*cb* construct in PIPES–NaOH pH 7.4 (25°C). Open and closed symbols correspond to independent experiments. The solid lines through the data points represent the best fittings to equation **4**. In the insets, the same data are presented as log/log plots, showing that the data obey equation **4** over the whole range of metal ion concentrations explored (50 μM–100 mM).

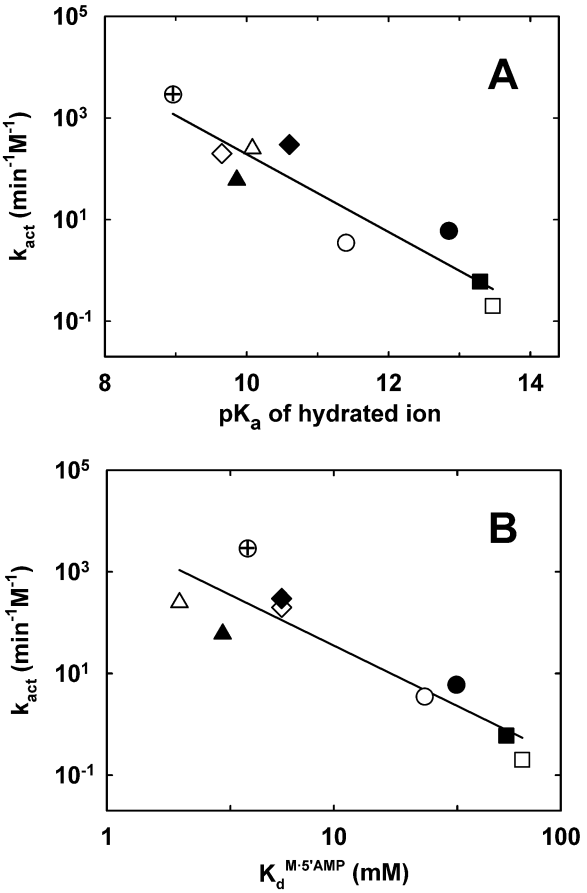

Figure 3. Correlations between k_{act} and some physico-chemical properties of the activating divalent metal ions (represented by different symbols: Mg^{2+}, open circles; Ca^{2+}, closed circles; Ba^{2+}, open squares; Sr^{2+}, closed squares; Co^{2+}, open diamonds; Mn^{2+}, closed diamonds; Cd^{2+}, open triangles; Ni^{2+}, closed triangles; Zn^{2+}, crossed circles). (**A**) Correlation between k_{act} and the pK_a of the hydrated metal ion. pK_a values were taken from Richens (47). The solid line represents a linear least-squares fit of the data, with slope = –0.76 ± 0.1 and R^2 = 0.87. (**B**) Correlation between k_{act} and the affinity of the metal ions for 5′AMP. The values of $K_d^{M\cdot 5'AMP}$ (the dissociation constant of the metal–5′AMP complex) were obtained from Massoud and Sigel (48). The solid line represents a linear least-squares fit of the data, with slope = –2.2 ± 0.4 and R^2 = 0.81.

8-17 reaction (11), their effect was not studied in this work. Pb^{2+} ions appear to promote catalysis through a peculiar two-step mechanism (25) and hence their mode of activation might be significantly different from that of all other ions cited above.

For most metal ions, complete titration curves of k_2 versus [M^{2+}] were not determined. Instead, to circumvent the scarce solubility of some metals at slightly alkaline pH and to limit the possibilities of metal-induced aggregation of DNA, k_2 was measured at a series of low [M^{2+}] values (usually <0.5 mM) where activity increased linearly with the metal ion concentration. The ability of each metal to activate the reaction was expressed by the slope of this line, k_{act} (= k_{max}/K_d). This is an apparent second-order rate constant for the activation, incorporating both binding of the metal ion and the subsequent cleavage step.

The order of effectiveness of the different metals was in good agreement with the data reported by Lu and coworkers (23), even though those authors employed a different 8-17 construct and a substrate containing a single ribonucleotide embedded in a DNA sequence. The measured k_{act} values showed correlations with some physico-chemical properties of the activating metal ion. In particular, k_{act} values appeared to be correlated with the acidity of the hydrated metal ion (Fig. 3A) and with the stability of the complexes that these metal ions form with nucleic acids (exemplified, in Fig. 3B, by AMP).

Dependence of k_2 on pH

The pH dependence of k_2 in the presence of either Mg^{2+} or Ca^{2+} was studied at 25°C, in Bis-tris propane–HCl buffer. The log of k_2 increased linearly with pH, up to pH ~8.5, with a slope of near unity (Fig. 4). An analogous linear pH-dependence of activity had been observed by Lu and

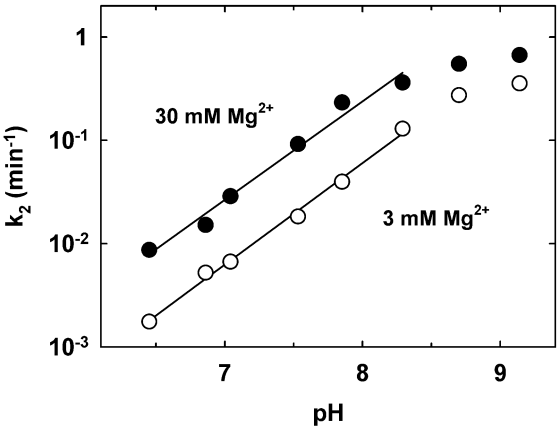

Figure 4. pH dependence of the rate of substrate cleavage. Single-turnover reactions were carried out at 25°C, in the presence of either 3 mM $MgCl_2$ (open circles) or 30 mM $MgCl_2$ (closed circles). The buffer used (50 mM Bis-tris propane–HCl) could cover the entire pH range 6.4–9.4, and its ionic strength was kept constant at 0.2 M by adding the appropriate amount of NaCl at each pH value. The solid lines represent linear least-squares fits of the data up to pH 8.5, and have slopes of 0.98 ± 0.1 (3 mM $MgCl_2$) and 0.95 ± 0.1 (30 mM $MgCl_2$). Nearly identical dependencies, with slopes of ~1.0 in the pH range 6.5–8.5, were observed for reactions carried out in 3 or 30 mM Ca^{2+} (data not shown).

coworkers under somewhat different conditions, in the pH range 5.7–7.4 (23). This log-linear behavior suggests that ionization of a single group within the E·S complex is required for catalysis. Most likely, this group can be identified with the 2′-hydroxyl of the adenosine residue at the cleavage site, which must be deprotonated in order to perform an efficient nucleophilic attack on the adjacent phosphorus center (34).

The deviation from linearity at pH >8.5 could mirror different phenomena. In principle, the leveling off of the rate might reflect complete deprotonation of the attacking 2′-hydroxyl group—in this case, the pK_a of this group within the E·S complex would be at least four units lower than normal (35). Nevertheless, it seems more reasonable to assume that deprotonation at other sites, within the deoxyribozyme core or even on the substrate-binding arms, could interfere with the chemical step at alkaline pH (36).

Dependence of k_2 on temperature

The rate of cleavage of the (8-17)*cb*–substrate complex, measured at pH 7.4 under various ionic conditions, increased ~100-fold between 0 and 37°C. However, the increase in rate with temperature was not linear over the entire temperature range explored, and the resulting Arrhenius plots showed a more or less pronounced curvature, which becomes evident at T >20°C (Fig. 5A). Very similar Arrhenius plots were obtained when using the (8-17)*q* construct (data not shown).

The linear part of the Arrhenius plots was fit to equation **5** (37), which relates the temperature dependence of a rate constant to the activation parameters (i.e. the differences in enthalpy and entropy between ground state and transition state) of the reaction:

$$\ln(k_2) = -\frac{\Delta H^{\ddagger}}{RT} + \frac{\Delta S^{\ddagger}}{R} + \ln\left(\frac{k_B T}{h}\right) \qquad \mathbf{5}$$

$\Delta H^{\ddagger}$ and $\Delta S^{\ddagger}$ are the enthalpy and the entropy of activation, respectively, for the cleavage step; T is the absolute temperature, R is the gas constant, k_B is Boltzmann's constant and h is Plank's constant. The apparent $\Delta H^{\ddagger}$ for the 8-17 reaction was found to lie in the range +27 to +28.7 kcal/mol. This is very close to the apparent $\Delta H^{\ddagger}$ values for the hammerhead ribozyme reaction in Mg^{2+} (+30.3 kcal/mol) (38) and for the non-enzymic RNA transesterification—the Arrhenius activation energy for this process is reportedly +29 kcal/mol (35), which corresponds to an apparent $\Delta H^{\ddagger}$ of +28.4 kcal/mol (37).

As for the observed curvature in the temperature dependence, non-linear Arrhenius plots are generally indicative of either some temperature-induced change in the reactants or of

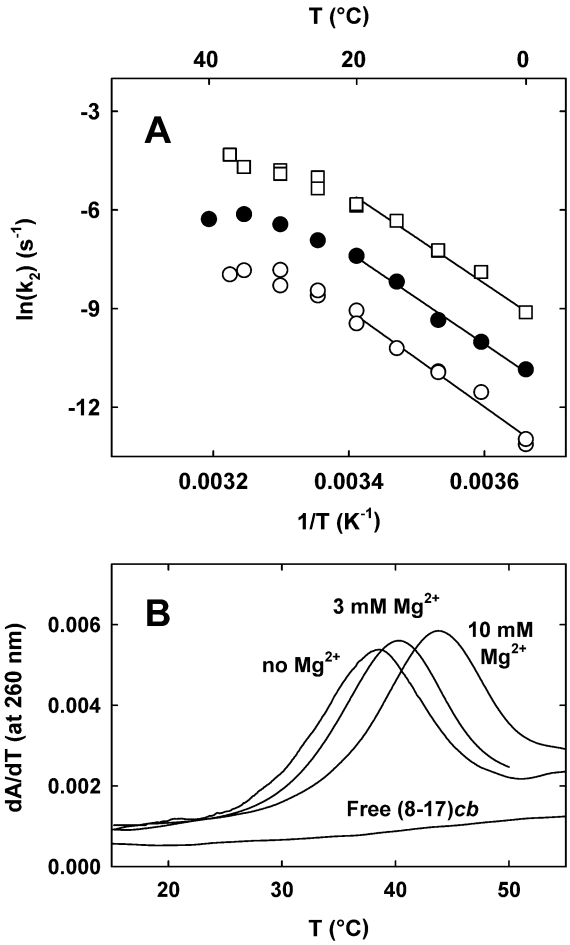

Figure 5. (**A**) Arrhenius plot of the (8-17)*cb* cleavage reaction in 3 mM Mg^{2+} (open circles), 100 mM Mg^{2+} (closed circles), or 3 mM Mn^{2+} (open squares) in PIPES–NaOH pH 7.4. Solid lines through the data points were obtained by fitting to equation **5** the data at T < 20°C. Bottom curve: $\Delta H^{\ddagger}$ = 28.7 kcal/mol and $\Delta S^{\ddagger}$ = 21 eu. Middle curve: $\Delta H^{\ddagger}$ = 27.2 kcal/mol and $\Delta S^{\ddagger}$ = 19.5 eu. Top curve: $\Delta H^{\ddagger}$ = 27 kcal/mol and $\Delta S^{\ddagger}$ = 22.4 eu. (**B**) Thermally induced melting of the complex formed by the (8-17)*cb* deoxyribozyme and a substrate analog containing a single deoxyribonucleotide at the cleavage site. The graphs represent the first derivative of UV absorption with respect to temperature. Deoxyribozyme and substrate analog were both present at 2 μM concentration. The original data fit well to a two-state melting transition, with ΔH^0 for association ranging from –90.9 kcal/mol (no Mg^{2+}) to –89.2 kcal/mol (10 mM Mg^{2+}) and ΔS^0 ranging from –266.3 eu (no Mg^{2+}) to –256 eu (10 mM Mg^{2+}); the calculated values of ΔG^0_{bind} at 25°C were –11.5 kcal/mol (no Mg^{2+}), –12.0 kcal/mol (3 mM Mg^{2+}) and –12.9 kcal/mol (10 mM Mg^{2+}). The derivative of the UV versus temperature profile for (8-17)*cb* (2 μM, no substrate analog added) is shown for comparison.

a change in the rate-limiting step of the reaction (38). In this case, however, a change in the rate-limiting step is unlikely: product release cannot be rate limiting at any temperature because reactions were single-turnover, while enzyme–substrate association cannot be rate-limiting because the observed reaction rates did not depend on the enzyme concentration. Therefore, the measured rates must reflect cleavage within the E·S complex.

In the case of the hammerhead ribozyme reaction, curved Arrhenius plots analogous to those in Figure 5A were tentatively explained by invoking a temperature-dependent transition in the ribozyme–substrate complex (38). By analogy, the effect of temperature on the 8-17 reaction seems also consistent with the occurrence of a conformational change of the E·S complex, occurring with a midpoint between 20 and 30°C. To test this possibility further, we carried out a UV melting study of a complex between (8-17)*cb* and a non-cleavable substrate analog (Fig. 5B). However, the study did not evidence any appreciable transition in the temperature range 20–30°C. This suggests that, if a conformational change occurs, it does not involve any significant melting of the helices present in the E·S complex—instead, it might include some pre-melting transition or a rearrangement in the deoxyribozyme tertiary structure.

DISCUSSION

A kinetic framework for the 8-17 reaction

We have analyzed the kinetic properties of a well behaved 8-17 construct, obtaining the multiple-turnover kinetic parameters for the deoxyribozyme reaction at two temperatures (37 and 25°C) and under different ionic conditions. At 25°C, we have also obtained the three main elemental rate constants in the deoxyribozyme kinetic mechanism: k_1, k_{-1} and k_2. Scheme 1 shows a summary of the kinetic constants for the (8-17)*cb* reaction in the presence of 3 mM Mg^{2+}, 25°C. A similar picture could be drawn for reaction in the presence of 3 mM Ca^{2+}.

A test of the consistency of these kinetic pictures is provided by their ability to predict the multiple turnover behavior of the (8-17)*cb* construct. In fact, comparison between the theoretical values for k_{cat} and K_M obtained from the application of equations **2** and **3** and the experimentally observed parameters supports the kinetic reconstruction. For example, based on the constants presented in Scheme 1, application of equation **3** would predict a K_M value of 2 nM, which is within 2-fold of the experimentally determined K_M.

Comparison with the 10-23 deoxyribozyme

The kinetic framework above permits a comparison of the properties of the 8-17 with the better known 10-23 deoxyribozyme. Indeed, while the 8-17 and 10-23 deoxyribozymes have been isolated during the same *in vitro* selection experiment, and described in the same publication (4), the 8-17 has been substantially less studied and less used for practical applications. In part, this may be due to the 10-23's greater flexibility in terms of target choice: the 10-23 construct can cleave an RNA phosphodiester bond located at any purine–pyrimidine site (22), whereas 8-17 requires an AG or GG site (23). Nevertheless, it is clear that the target specificities of the two constructs are complementary, rather than alternative.

The 10-23 was originally described as catalytically more active than the 8-17 motif (4), but some subsequent, limited studies hinted that the difference in cleavage rate between the two constructs may be minimal (39,40). The present study reinforces this view, as the k_{cat} values measured herein are similar to k_{cat} (or k_2) values measured for 10-23 constructs under analogous reaction conditions (15,22,30).

The two deoxyribozymes can be compared also on the basis of their specificity constants (k_{cat}/K_M), which reflect catalytic performance at subsaturating substrate concentrations (15). For the (8-17)*cb* construct, k_{cat}/K_M under simulated physiological conditions (37°C, 3 mM Mg^{2+} pH 7.4) was 4×10^5 M^{-1} min^{-1}—strikingly less than the value of 3.2×10^8 M^{-1} min^{-1} reported for an optimized version of the 10-23 DNAzyme, under similar conditions (15). This dramatic difference must not be taken at face value, however. k_{cat}/K_M depends largely on the stability of the complex between deoxyribozyme and substrate, and hence on the length and composition of the substrate-binding 'arms', as well as on temperature. In fact, for the (8-17)*cb* construct, k_{cat}/K_M values measured at 25°C ranged between 2×10^6 and 10^7 M^{-1} min^{-1} and were thus substantially larger than the values measured at 37°C. Note also that the observed k_{cat}/K_M values for the (8-17)*q* construct were systematically larger than the values for the (8-17)*cb* construct, in accord with the greater affinity of the former deoxyribozyme for its substrate. These observations indicate that k_{cat}/K_M in the 8-17 system can be modulated and improved by increasing substrate affinity—in practical applications, this may be achieved for example by elongating the substrate-binding arms.

Yet there is a limit to such improvements: at most, k_{cat}/K_M can be as great as k_1, the rate constant for association of the DNAzyme with its substrate (16). k_1 for both the (8-17)*cb* and the (8-17)*q* constructs lies in the range $1–5 \times 10^7$ M^{-1} min^{-1}, which is about one order of magnitude slower than substrate binding by the 10-23 deoxyribozyme and also than the annealing rates typical of small complementary oligonucleotides (15). All this means that even an optimized 8-17 construct should not be able to match the k_{cat}/K_M values described in the 10-23 system.

Why is substrate binding by the 8-17 deoxyribozyme relatively slow in comparison with the 10-23 motif? The similar values of k_1 determined for two different 8-17 constructs make it unlikely that the observed binding rates depend on the existence of alternative secondary structures

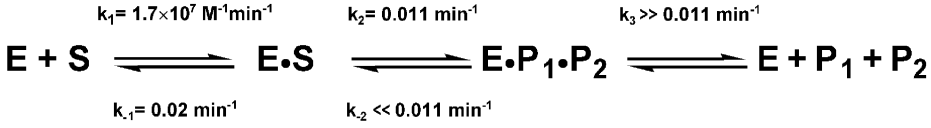

Scheme 1.

involving the deoxyribozyme arms. It is possible, however, that binding of the substrate is accompanied by some structural rearrangement of the central 'core' region, which may limit the overall process. In this respect, it should be noted that the rates of substrate binding measured in this study are similar to those reported for the hammerhead ribozyme (28)—an RNA enzyme whose catalytic core contains an intramolecular stem, as observed with the 8-17 deoxyribozyme.

Estimating the 'core energetic penalty' for substrate binding

Attainment of the kinetic constants k_1 and k_{-1} allows calculation of the thermodynamic constant for substrate dissociation ($K_S = k_{-1}/k_1$) and hence the free energy of substrate binding (ΔG^0_{bind}):

$$\Delta G^0_{bind} = RT \ln(K_S) \quad \mathbf{6}$$

The observed ΔG^0_{bind} values are approximately –12.0 kcal/mol for the (8-17)*cb* construct (this value is fully consistent with the results of thermal denaturation analysis; Fig. 5B) and –13.4 kcal/mol for the (8-17)*q* construct. These observed free energy changes are the result of at least two contributions, namely: (i) the favorable free energy for formation of the two heteroduplexes between the deoxyribozyme arms and the substrate ($\Delta G^0_{helices}$) and (ii) the unfavorable free energy ('energetic penalty') attributable to the presence of the deoxyribozyme core, which interrupts the substrate binding helices (ΔG^0_{core}). The latter contribution is particularly important, because establishment of a constant 'core energetic penalty' would substantially help the rational design of deoxyribozymes directed toward specific RNA targets (41).

Reliable estimates for $\Delta G^0_{helices}$ can be obtained through the application of nearest-neighbor parameters. In particular, we calculated $\Delta G^0_{helices}$ as the sum of the free energies for both helices, derived from the empirically determined free energies for DNA–RNA base pairings (42), corrected by a single bimolecular initiation penalty (ΔG^0_i = +3.1 kcal/mol). The 'core energetic penalty' can then be calculated as:

$$\Delta G^0_{core} = \Delta G^0_{bind} - \Delta G^0_{helices} \quad \mathbf{7}$$

For both constructs, the values of ΔG^0_{core} obtained through this calculation approach +7 kcal/mol. In rigorous terms, this number must be considered an overestimate, as the nearest-neighbor parameters refer to the stability of basepairs at 1 M ionic strength (42), whereas we measured ΔG^0_{bind} at ~0.21 M ionic strength. Nonetheless, observation of a constant 'core energetic penalty' in two different constructs strongly suggests that the 8-17 core provides a uniform thermodynamic contribution to substrate binding. If the occurrence of such a constant 'energetic penalty' is confirmed by analysis of other 8-17 systems, containing e.g. arms of different lengths, this would permit the easy prediction of substrate binding affinities for any 8-17 deoxyribozyme–substrate pair.

A single activating metal ion?

After binding of the substrate to the deoxyribozyme, cleavage requires the presence of divalent metal ions. We have measured activation of the 8-17 deoxyribozyme by Mg^{2+}, Ca^{2+} and Mn^{2+}, showing that in each case activation can be described by a single, non-cooperative (hyperbolic) process. Hyperbolic dependences like the ones described here had been reported previously by Lu and coworkers, who employed different metal ions, such as Zn^{2+}, and a different 8-17 construct (23,25). The simplest and most straightforward interpretation of these data is that just one metal ion, binding at a single, low-specificity site within the E·S complex, is required to bring about catalysis.

This conclusion is surprising, given the large number of metal ions expected to bind to the negatively charged 8-17 system. Indeed, one can envisage more complex kinetic models in which two (or more) metal ions are required for activity, and yet the dependence of k_2 on metal concentration is indistinguishable from that expected for a single activating ion. For example, if one metal ion were bound tightly (K_d < 50 μM) to the E·S complex, but did not provide a significant rate enhancement until a second metal ion bound at a lower affinity site, the dependence of activity on $[M^{2+}]$ would be hyperbolic. In this case the observed K_d would reflect binding of the second metal ion, pivotal for the activation process.

What is the location of the binding site for the activating metal ion? A reasonable hypothesis is that the metal ion cofactor binds to the unpaired region at the 3′ end of the core (TCGAA). We reported previously that mutations in this stretch of nucleotides modulate the relative activating efficiency of different metals (24). Furthermore, preliminary spectroscopic data suggest that binding of metal ions induces a conformational change in this loop, and that this conformational change is concomitant with activation (our unpublished results). Binding of an ion near the junction between the three helices of the E·S complex seems also consistent with the results of FRET studies, which indicate that in the presence of divalent metal ions the three helices rearrange along the edges of a pyramid (43).

Metal ions and the mechanism of the 8-17 deoxyribozyme

In a recent paper, Breaker and coworkers have outlined schematically what catalytic strategies can be adopted by RNA-cleaving ribozymes and deoxyribozymes, and therefore what roles could be played by metal ions in the reaction mechanism of these catalysts (44). These roles include neutralization of the negative charge on a non-bridging oxygen of the phosphodiester linkage ('β strategy'), assistance in the deprotonation of the 2′-hydroxyl group at the cleavage site ('γ strategy') and stabilization of the negatively charged 5′-oxygen leaving group ('δ strategy').

The rate of substrate cleavage by the 8-17 DNA enzyme is influenced by both pH and the nature of the divalent metal ion used as a cofactor. In particular, as shown in Figure 3A, the observed k_{act} values showed a strong correlation with the pK_a of the hydrated metal ion cofactor. A similar behavior had been described earlier for the hammerhead ribozyme (45) and for the 10-23 deoxyribozyme (15,18), and interpreted as evidence that the chemical mechanism of these catalysts involves a metal-assisted deprotonation of the reactive 2′-hydroxyl as part of the rate-limiting step ('γ strategy'). For example, a metal-bound hydroxide could function as a general base to deprotonate the 2′-hydroxyl group (in that case, Fig. 3A

would represent a true Brönsted plot for the transesterification reaction). Another hypothesis is that the metal ion could act as a Lewis acid, coordinating directly to the 2′-hydroxyl and aiding its deprotonation (18).

While these hypotheses remain fully plausible, we would like to signal a more general interpretation of the data. Formally, according to transition state theory, the parameter k_{act} reflects the affinity of a given metal ion for the transition state of the 8-17 reaction: the metal ions that are better activators of the 8-17 deoxyribozyme are those that better stabilize the transition state. Put another way, differences in k_{act} between metal ions are expected to mirror the relative strength of the interactions that these ions form with the E·S complex in the transition state. As a matter of fact, the k_{act} values measured for different metal ions show an appreciable correlation with the relative affinities of these ions for nucleic acids (Fig. 3B).

This observation stresses that the activating metal ion may not be necessarily involved in a 'γ strategy' mechanism, acting as a Lewis acid or as a general base. It could as well promote catalysis by interacting with the non-bridging oxygen and/or with the leaving group ['β strategy' and 'δ strategy', respectively, according to the nomenclature proposed in Breaker *et al.* (34)], without being involved in the 2′-hydroxyl deprotonation process. In principle, the crucial metal ion could even play a purely structural role, helping to stabilize a reactive conformation of the E·S complex. This ambiguity is intrinsic to the analysis of metal-ion activation effects, since those metal ions that are stronger Lewis acids are also capable of forming stronger interactions with liganding groups such as the phosphate oxygens. More specific experiments will be required to address the exact role of metal ions in the activation process.

Conclusions

The 8-17 deoxyribozyme is one of the simplest RNA-cleaving DNA motifs discovered to date. It binds its substrate with a rate analogous to that of the well known hammerhead ribozyme, and it performs catalysis only in the presence of divalent metal ions. Activation appears to depend on the occupation of a single, low-specificity binding site. The direct involvement of the activating metal ion in the chemical step of the reaction is plausible, but additionally or alternatively, a structural role cannot be excluded. Indeed, Liu and Lu have recently shown that in the 8-17 system metal binding is coupled to global conformational changes, even though the relationship between these conformational changes and activation is unclear (43).

A possible structural role of the activating metal ion could be the alignment and positioning of catalytic and reacting groups at the cleavage site. Precise alignment of reactive groups is a hallmark of biological catalysts (46) and even if the 8-17 is small and very inefficient compared with most natural protein and RNA enzymes, it may be able to achieve, at least in part, such preorganization. This possibility is consistent with our temperature dependence data. In fact, as noted above, the apparent enthalpy of activation for the 8-17 reaction is very close to the enthalpy of activation for the hydroxide-catalyzed RNA cleavage (which is about six orders of magnitude slower under our reaction conditions). Even though one must be very cautious in interpreting the apparent activation parameters of biochemical processes (38), this coincidence hints that the large difference in rate between the two transesterification reactions may be dictated almost only by entropic factors.

ACKNOWLEDGEMENTS

We thank R.Corradini for help with the thermal denaturation measurements. This work was supported by a grant from the EMBO Young Investigator Programme (to A.P.).

REFERENCES

1. Gold,L., Polisky,B., Uhlenbeck,O. and Yarus,M. (1995) Diversity of oligonucleotide functions. *Annu. Rev. Biochem.*, **64**, 763–797.
2. Breaker,R.R. (1997) DNA aptamers and DNA enzymes. *Curr. Opin. Chem. Biol.*, **1**, 26–31.
3. Sen,D. and Geyer,C.R. (1998) DNA enzymes. *Curr. Opin. Chem. Biol.,* **2**, 680–687.
4. Santoro,S.W. and Joyce,G.F. (1997) A general purpose RNA-cleaving DNA enzyme. *Proc. Natl Acad. Sci. USA*, **94**, 4262–4266.
5. Khachigian,L.M. (2000) Catalytic DNAs as potential therapeutic agents and sequence-specific molecular tools to dissect biological function. *J. Clin. Invest.*, **106**, 1189–1195.
6. Cairns,M.J., Saravolac,E.G. and Sun,L.Q. (2002) Catalytic DNA: a novel tool for gene suppression. *Curr. Drug Targets*, **3**, 269–279.
7. Todd,A.V., Fuery,C.J., Impey,H.L., Applegate,T.L. and Haughton,M.A. (2000) DzyNA-PCR: use of DNAzymes to detect and quantify nucleic acid sequences in a real-time fluorescent format. *Clin. Chem.*, **46**, 625–630.
8. Cairns,M.J., King,A. and Sun,L.Q. (2000) Nucleic acid mutation analysis using catalytic DNA. *Nucleic Acids Res.*, **28**, e9.
9. Pyle,A.M., Chu,V.T., Jankowsky,E. and Boudvillain,M. (2000) Using DNAzymes to cut, process and map RNA molecules for structural studies or modification. *Methods Enzymol.*, **317**, 140–146.
10. Sohail,M., Doran,G., Riedemann,J., Macaulay,V. and Southern,E.M. (2003) A simple and cost-effective method for producing small interfering RNAs with high efficacy. *Nucleic Acids Res.*, **31**, e38.
11. Li,J. and Lu,Y. (2000) A highly sensitive and selective catalytic DNA biosensor for lead ions. *J. Am. Chem. Soc.*, **122**, 10466–10467.
12. Liu,J. and Lu,Y. (2003) A colorimetric lead biosensor using DNAzyme-directed assembly of gold nanoparticles. *J. Am. Chem. Soc.*, **125**, 6642–6643.
13. Stojanovic,M.N., Mitchell,T.E. and Stefanovic,D. (2002) Deoxyribozyme-based logic gates. *J. Am. Chem. Soc.*, **124**, 3555–3561.
14. Stojanovic,M.N. and Stefanovic,D. (2003) Deoxyribozyme-based half-adder. *J. Am. Chem. Soc.*, **125**, 6673–6676.
15. Santoro,S.W. and Joyce,G.F. (1998) Mechanism and utility of an RNA-cleaving DNA enzyme. *Biochemistry*, **37**, 13330–13342.
16. Joyce,G.F. (2001) RNA cleavage by the 10-23 DNA enzyme. *Methods Enzymol.*, **341**, 503–517.
17. Ota,N., Warashina,M., Hirano,K., Hatanaka,K. and Taira,K. (1998) Effects of helical structures formed by the binding arms of DNAzymes and their substrates on catalytic activity. *Nucleic Acids Res.*, **26**, 3385–3391.
18. He,Q.C., Zhou,J.M., Zhou,D.M., Nakamatsu,Y., Baba,T. and Taira,K. (2002) Comparison of metal-ion-dependent cleavages of RNA by a DNA enzyme and a hammerhead ribozyme. *Biomacromolecules*, **3**, 69–83.
19. Cairns,M.J., Hopkins,T.M., Witherington,C. and Sun,L.Q. (2000) The influence of arm length asymmetry and base substitution on the activity of the 10-23 DNA enzyme. *Antisense Nucleic Acid Drug Dev.*, **10**, 323–332.
20. Horn,S. and Schwenzer,B. (1999) Oligonucleotide facilitators enhance the catalytic activity of RNA-cleaving DNA enzymes. *Antisense Nucleic Acid Drug Dev.*, **9**, 465–472.
21. Kurreck,J., Bieber,B., Jahnel,R. and Erdmann,V.A. (2002) Comparative study of DNA enzymes and ribozymes against the same full-length messenger RNA of the vanilloid receptor subtype I. *J. Biol. Chem.*, **277**, 7099–7107.
22. Cairns,M.J., King,A. and Sun,L.Q. (2003) Optimisation of the 10-23 DNAzyme–substrate pairing interactions enhanced RNA cleavage

activity at purine-cytosine target sites. *Nucleic Acids Res.*, **31**, 2883–2889.
23. Li,J., Zheng,W., Kwon,A.H. and Lu,Y. (2000) *In vitro* selection and characterization of a highly efficient Zn(II)-dependent RNA-cleaving deoxyribozyme. *Nucleic Acids Res.*, **28**, 481–488.
24. Peracchi,A. (2000) Preferential activation of the 8-17 deoxyribozyme by Ca^{2+} ions. Evidence for the identity of 8-17 with the catalytic domain of the Mg5 deoxyribozyme. *J. Biol. Chem.*, **275**, 11693–11697.
25. Brown,A.K., Li,J., Pavot,C.M.-B. and Lu,Y. (2003) A lead-dependent DNAzyme with a two-step mechanism. *Biochemistry*, **42**, 7152–7161.
26. Cantor,C.R., Warshaw,M.M. and Shapiro,H. (1970) Oligonucleotide interactions. III. Circular dichroism studies of the conformation of deoxyoligonucleotides. *Biopolymers*, **9**, 1059–1077.
27. Fedor,M.J. and Uhlenbeck,O.C. (1990) Substrate sequence effects on 'hammerhead' RNA catalytic efficiency. *Proc. Natl Acad. Sci. USA*, **87**, 1668–1672.
28. Hertel,K.J., Herschlag,D. and Uhlenbeck,O.C. (1994) A kinetic and thermodynamic framework for the hammerhead ribozyme reaction. *Biochemistry*, **33**, 3374–3385.
29. Fersht,A. (1985) *Enzyme Structure and Mechanism*. Freeman & Co., New York, NY, pp. 137–138.
30. Ferrari,D. and Peracchi,A. (2002) A continuous kinetic assay for RNA-cleaving deoxyribozymes, exploiting ethidium bromide as an extrinsic fluorescent probe. *Nucleic Acids Res.*, **30**, e112.
31. Flynn-Charlebois,A., Prior,T.K., Hoadley,K.A. and Silverman,S.K. (2003) *In vitro* evolution of an RNA-cleaving DNA enzyme into an RNA ligase switches the selectivity from 3′-5′ to 2′-5′. *J. Am. Chem. Soc.*, **125**, 5346–5350.
32. Segel,I.H. (1975) *Enzyme Kinetics*. John Wiley & Sons, New York, NY.
33. Murray,J.B., Seyhan,A.A., Walter,N.G., Burke,J.M. and Scott,W.G. (1998) The hammerhead, hairpin and VS ribozymes are catalytically proficient in monovalent cations alone. *Chem. Biol.*, **5**, 587–595.
34. Breaker,R.R., Emilsson,G.M., Lazarev,D., Nakamura,S., Puskarz,I.J., Roth,A. and Sudarsan,N. (2003) A common speed limit for RNA-cleaving ribozymes and deoxyribozymes. *RNA*, **9**, 949–957.
35. Li,Y. and Breaker,R. (1999) Kinetics of RNA degradation by specific base catalysis of transesterification involving the 2′-hydroxyl group. *J. Am. Chem. Soc.*, **121**, 5364–5372.
36. Knitt,D.S. and Herschlag,D. (1996) pH dependencies of the *Tetrahymena* ribozyme reveal an unconventional origin of an apparent pK_a. *Biochemistry*, **34**, 1560–1570.
37. Walmsley,A.R. (1996) The effect of temperature on enzyme-catalysed reactions. In Engel,P.C. (ed.), *Enzymology Labfax*. Academic Press, San Diego, pp. 175–198.
38. Peracchi,A. (1999) Origins of the temperature dependence of hammerhead ribozyme catalysis. *Nucleic Acids Res.*, **27**, 2875–2882.
39. Kuwabara,T., Warashina,M., Tanabe,T., Tani,K., Asano,S. and Taira,K. (1997) Comparison of the specificities and catalytic activities of hammerhead ribozymes and DNA enzymes with respect to cleavage of BCR-ABL chimeric L6 (b2a2) mRNA. *Nucleic Acids Res.*, **25**, 3074–3081.
40. Chakraborti,S. and Banerjea,A.C. (2003) Identification of cleavage sites in the HIV-1 TAR RNA by 10-23 and 8-17 catalytic motif containing DNA enzymes. *Biomacromolecules*, **4**, 568–571.
41. Hertel,K.J., Stage-Zimmermann,T.K., Ammons,G. and Uhlenbeck,O.C. (1998) Thermodynamic dissection of the substrate–ribozyme interaction in the hammerhead ribozyme. *Biochemistry*, **37**, 16983–16988.
42. Sugimoto,N., Nakano,S., Katoh,M., Matsumura,A., Nakamuta,H., Ohmichi,T., Yoneyama,M. and Sasaki,M. (1995) Thermodynamic parameters to predict stability of RNA/DNA hybrid duplexes. *Biochemistry*, **34**, 11211–11216.
43. Liu,J. and Lu,Y. (2002) FRET study of a trifluorophore-labeled DNAzyme. *J. Am. Chem. Soc.*, **124**, 15208–15216.
44. Emilsson,G.M., Nakamura,S., Roth,A. and Breaker,R.R. (2003) Ribozyme speed limits. *RNA*, **9**, 907–918.
45. Dahm,S.C., Derrick,W.B. and Uhlenbeck,O.C. (1993) Evidence for the role of solvated metal hydroxide in the hammerhead cleavage mechanism. *Biochemistry*, **32**, 13040–13045.
46. Kraut,D.A., Carroll,K.S. and Herschlag,D. (2003) Challenges in enzyme mechanism and energetics. *Annu. Rev. Biochem.*, **72**, 517–571.
47. Richens,D. (1997) *The Chemistry of Aqua Ions*. John Wiley & Sons, New York, NY.
48. Massoud,S.S. and Sigel,H. (1989) Evaluation of the metal-ion-coordinating differences between the 2′-, 3′- and 5′-monophosphates of adenosine. *Eur. J. Biochem.*, **179**, 451–458.